ISSN 1070-4272, Russian Journal of Applied Chemistry, 2020, Vol. 93, No. 8, pp. 1132–1138. © Pleiades Publishing, Ltd., 2020.
Russian Text © The Author(s), 2020, published in Zhurnal Prikladnoi Khimii, 2020, Vol. 93, No. 8, pp. 1098–1104.

INORGANIC SYNTHESIS AND INDUSTRIAL INORGANIC CHEMISTRY

Synthesis and Physicochemical Properties of Complex Oxides $K_2Me_xTi_{8-x}O_{16}$ (Me = Mg, Ni, Al) of Hollandite Structure

N. V. Besprozvannykh[a,*], O. Yu. Sinel'shchikova[a,], N. A. Morozov[a], S. K. Kuchaeva[a], and A. Yu. Postnov[b]**

[a] *Grebenshchikov Institute of Silicate Chemistry, Russian Academy of Sciences, St. Petersburg, 199034 Russia*
[b] *St. Petersburg State Institute of Technology (Technical University), St. Petersburg, 190015 Russia*
**e-mail: besprozvannykh.nv@gmail.com*
***e-mail: sinelshikova@mail.ru*

Received December 13, 2019; revised February 24, 2020; accepted May 27, 2020

Abstract—Materials of the hollandite structure in the K_2O–$MeO(Me_2O_3)$–TiO_2 (Me = Al, Ni, Mg) system, synthesized by two methods (solid-phase synthesis and pyrolysis of citrate–nitrate compositions), were studied. The pyrolysis, compared to the traditional solid-phase synthesis, yielded the materials with the more developed specific surface and, as a consequence, enhanced performance in sorption of a model dye, Methylene Blue (for $K_2MgTi_7O_{16}$, q = 18.75 mg g^{-1}). The $K_2Al_2Ti_6O_{16}$ sample, also prepared by pyrolysis, showed the highest catalytic performance in oxidation of CO and H_2. The hydrogen oxidation on this catalyst occurred to 95% at 355°C with the performance of ~0.21×10^{-5} mol g^{-1} s^{-1}, which is two times higher compared to the sample of the same composition prepared by the solid-phase method. The hollandites show promise as sorbents and catalysts for gas treatment.

Keywords: hollandites, sorption, photocatalysis, oxidation of CO and H_2, band gap

DOI: 10.1134/S1070427220080042

Adsorption followed by heterogeneous photocatalysis is one of the most promising processes used in wastewater treatment to remove organic pollutants. Today titanium dioxide is one of the most actively used and studied material for this purpose. Numerous recent studies were aimed at enhancing its photocatalytic activity by varying the TiO_2 synthesis conditions to obtain materials with a more developed surface [1], by doping with various elements [2, 3], and by preparing complex oxides [4–7]. These approaches allow the absorption of the electromagnetic radiation to be shifted to the visible range of the solar spectrum and the probability of electron–hole recombination to be reduced by the formation of heterotransitions.

The photocatalytic activity of complex titanates of hollandite-type structure has been studied insufficiently, despite structural features allowing wide variation of their composition. However, the published papers [8, 9] demonstrate the urgency of studying the photocatalytic and optical properties of compounds of this type. It should also be noted that particles of potassium magnesium titanate of hollandite-type structure, prepared by crystallization from molten salts, exhibit high reflection coefficient in the near-IR range, which is important for refractory materials and heat-reflecting coatings [10].

Ceramics based on a series of hollandite phases exhibit low electrical conductivity at room temperature and relatively high K-ionic conductivity in the range 700–1000°C, accompanied for some compositions by an abnormally strong increase in the dielectric permittivity [11–14]. In opinion of Gorshkov et al. [11], this combination of properties makes the ceramics based on hollandite phases promising for the development of thermoelectric thermal energy converters allowing not only generation of the electric power by absorption of heat emitted by industrial furnaces but also accumulation of the electric power for the subsequent use (ceramic supercapacitor).

The use of titanates of the hollandite group as heterogeneous catalysts is also interesting. A series of these complex oxides were tested in oxidation of C, CO, and H_2 and in reduction of NO_x in the presence of hydrocarbons [15–18].

This study was aimed at revealing the relationship between the composition, synthesis method, and functional physicochemical properties of complex oxides of hollandite-type structure, crystallizing in the K_2O–MeO (Me_2O_3)–TiO_2 (Me = Al, Ni, Mg) system, to determine the prospects for using materials based on them.

EXPERIMENTAL

The samples were prepared by the (a) solid-phase method and (b) pyrolysis of citrate–nitrate compositions.

In the first case, the starting mixture was prepared from the following carbonates and oxides: K_2CO_3 (chemically pure grade), Al_2O_3 (ultrapure grade), $NiCO_3$ (pure grade), $MgCO_3$ (ultrapure grade), and TiO_2 (ultrapure grade). The starting reactants were ground and mixed manually. The metal ratio corresponded to the stoichiometry of the desired titanate: $K_2Me_xTi_{8-x}O_{16}$, where $x = 2$ at Me = Al и $x = 1$ at Me = Mg, Ni. The resulting charge was pressed at 100 MPa and sintered stepwise at 1000 and 1100°C. The charge for preparing the aluminum-containing hollandite was subjected to the third sintering at 1250°C. The heat treatment time in each step was 6 h.

The starting citrate–nitrate compositions for pyrolysis were prepared as described in [18]. The following chemicals were taken for preparing the starting solutions: KNO_3 (ultrapure grade), $Al(NO_3)_3 \cdot 9H_2O$ (ultrapure grade), MgO (ultrapure grade), $Ni_3(OH)_4CO_3 \cdot 4H_2O$ (chemically pure grade), and $TiCl_4$ (ultrapure grade). The magnesium nitrate solution was prepared by the reaction of MgO with dilute HNO_3 (ultrapure grade); nickel was introduced in the form of a citrate solution prepared by the reaction of basic nickel carbonate with citric acid ($C_6H_8O_7 \cdot H_2O$, ultrapure grade).

As in the solid-phase synthesis, the metal ratio corresponded to the synthesis stoichiometry. The required volume of citric acid was calculated from the amount of NO_3 groups in the nitrate components. The following relationship should be observed to ensure complete reduction of nitrogen in nitrates:

$$n = 5(\sum NO_3)/m,$$

where n is the number of moles of the reductant per mole of the product, and m is the number of bonds being oxidized in one molecule of the organic substance (for citric acid, $m = 20$).

In the course of the experiment, we prepared compositions with the reductant amount equal to the calculated value, i.e., with the nominal reductant to oxidant ratio $\varphi = 1.0$.

After dissolving the mixture in citric acid, the mixture was adjusted to pH 6.5 with a highly dilute aqueous ammonia solution. This led to the formation of a sol, which transformed into a gel in the course of evaporation at 80°C. The powders of hollandite phases were prepared by combustion followed by heat treatment of the gels at 650°C for 1–2 h.

The samples in different steps of the synthesis were analyzed by X-ray diffraction (XRD) with a DRON-3M diffractometer using Cu_{K_α} radiation. The pore structure was studied by low-temperature nitrogen sorption (Quantachrome NOVA 1200e, the United States). The samples were degassed at 300°C for 0.5 h. The specific surface area (S_{sp}) of the samples was calculated by the Brunauer–Emmett–Teller (BET) method.

The band structure parameters of the samples obtained, including the band gap width (E_g), were determined by mathematical processing of diffuse reflection spectra recorded in the range 220–850 nm with a Shimadzu UV2600 UV spectrometer equipped with an integrating sphere. Measurements were performed using compacted powder samples. The band gap width E_g was determined by extrapolation of the linear portions of the Kubelka–Munk function $F(E)$ to the interception with the E-axis:

$$F(E) = (1 - R)^2/2R,$$

where R is the diffuse reflection coefficient and $E = hc/\lambda$ is the light quantum energy (eV).

The catalytic activity of the samples in the model reactions of the CO ($c_0 = 2$ vol %) and H_2 ($c_0 = 3$ vol %) oxidation was studied in flow-through installations. The volume of granules (fraction 1–2 mm) prepared by pressing the starting compositions was 2–3 cm^3, and the flow rate of the gas–air mixture was $V = 3.3$ cm^3 s^{-1}. The mixture was analyzed with a Tsvet-500 chromatograph.

The productivity in the CO (H_2) oxidation per gram of the catalyst, [mol CO (H_2)] s^{-1} g^{-1}, was calculated using the equation

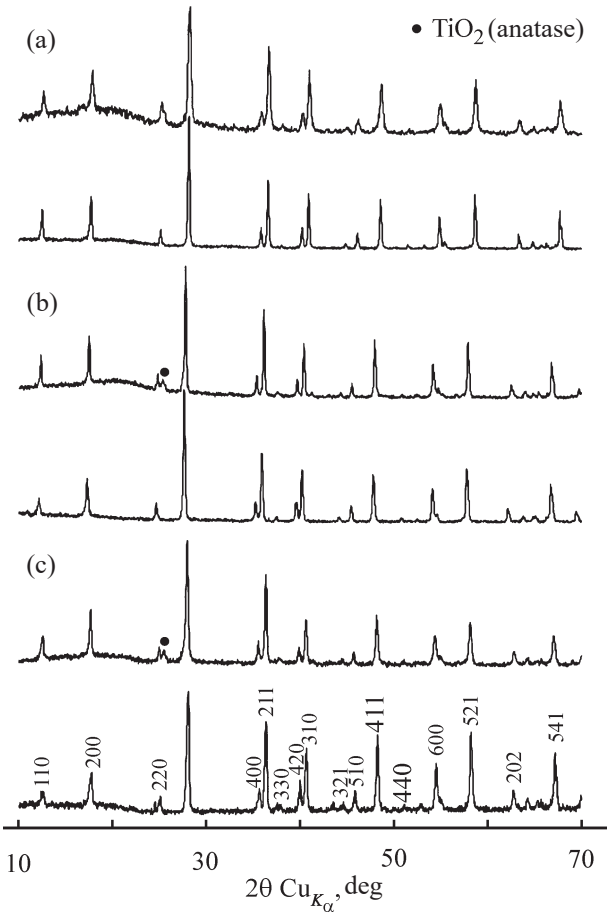

Fig. 1. Diffraction patterns of (a) $K_2Al_2Ti_6O_{16}$, (b) $K_2MgTi_7O_{16}$, and (c) $K_2NiTi_7O_{16}$ samples prepared by (lower plot) solid-phase method and (upper plot) pyrolysis of citrate–nitrate compositions.

$$P_m = Vc_0x/22.4m,$$

where x is the conversion (volume fraction); 22.4, molar volume (dm^3 mol^{-1}); m, catalyst weight (g); c_0, initial concentration of the gas being oxidized (volume fraction); and V, flow rate of the gas–air mixture (dm^3 s^{-1}).

To study the sorption capacity of the materials for organic dyes, we chose Methylene Blue as a model dye. The initial Methylene Blue solution was prepared so as to obtain the minimal light transmittance value recorded with the spectrophotometer used (PE-5400 UF); it corresponded to a concentration of 210 mg L^{-1}. A 5-mL portion of the dye solution was transferred into a 10-mm-thick cell containing a sorbent sample (0.015 g). Immediately after that, the cell was arranged in the spectrophotometer, and the transmittance was recorded for 60 min at 2-s intervals. The data obtained were processed using the preliminarily constructed calibration plots.

The electrophysical properties, including the imaginary and real parts of the complex resistance (Z'', Z') and the total electrical conductivity σ, were determined with a Z-2000 impedance meter using a two-electrode scheme in the frequency range from 1 Hz to 2 MHz with the measuring signal amplitude of 125 mV in the temperature interval 600–700°C. The contacts were deposited onto the ceramic samples in the form of a conducting silver paste (produced by Elma Pasta) and annealed at 700°C for 4 h.

RESULTS AND DISCUSSION

According to the X-ray diffraction data (Fig. 1), the majority of the materials obtained are single-phase and have the crystal structure of the hollandite type ($K_{1.35}Ti_8O_{16}$, PDF 47-0690 card of the Powder Diffraction File). However, the magnesium- and nickel-containing samples prepared by the citrate–nitrate method have a small impurity of titanium oxide in the anatase form.

When using materials in sorption, catalysis, and some electrochemical processes, the specific surface

Table 1. Specific surface area of samples prepared by different methods

Stoichiometric composition	Synthesis method	Specific surface area, m^2 g^{-1}
$K_2NiTi_7O_{16}$	Solid-phase	0.268
$K_2MgTi_7O_{16}$		1.718
$K_2Al_2Ti_6O_{16}$		1.148
$K_2NiTi_7O_{16}$	Citrate–nitrate	11.529
$K_2MgTi_7O_{16}$		11.128
$K_2Al_2Ti_6O_{16}$		12.457

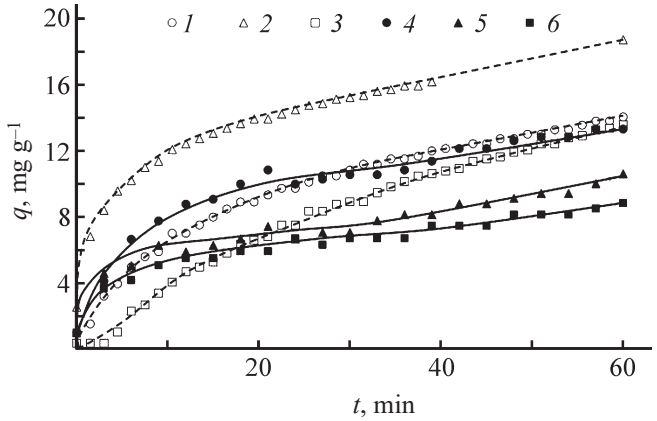

Fig. 2. Kinetic curves of sorption of Methylene Blue onto (*1*, *4*) $K_2NiTi_7O_{16}$, (*2*, *5*) $K_2MgTi_7O_{16}$, and (*3*, *6*) $K_2Al_2Ti_6O_{16}$ samples prepared by the (solid lines) solid-phase method and (dashed lines) pyrolysis of citrate–nitrate compositions.

area is one of the key factors associated with the heterogeneous character of the processes. In this study, the pyrolysis of the citrate–nitrate compositions as the synthesis procedure allowed the specific surface area to be increased only to ~10 $m^2\ g^{-1}$ (Table 1).

Nevertheless, the hollandite structure, which is a framework of metal–oxygen octahedra, pierced in one of the directions by "tunnels" accommodating large mono- or bivalent cations, allows these compounds to be considered as a kind of molecular sieves. At low specific surface areas, the surface phenomena will largely depend on the physicochemical state of the surface, in particular, on the crystal lattice defectiveness, presence of coordination-unsaturated cations, and acid–base properties. These factors influence the dye sorption. The Mg- and Al-containing ceramic materials prepared by the citrate–nitrate method exhibit approximately 2 times higher sorption activity compared to the samples prepared by solid-phase reactions (Fig. 2, curves *2* and *3* compared to *5* and *6*, respectively). In the case of the nickel hollandite, however, the use of pyrolysis of citrate–nitrate compositions does not lead to an increase in the sorption capacity. It should be noted that the use of this method decreases the sorption rate in the initial period (Fig. 2, curves *1* and *4*).

Trials of the catalysts in the model processes have shown (Fig. 3) that the CO oxidation on all the hollandites occurs at moderately high temperatures, 250–540°C, and the hydrogen oxidation occurs at temperatures from 60 to 350°C. The use of pyrolysis of

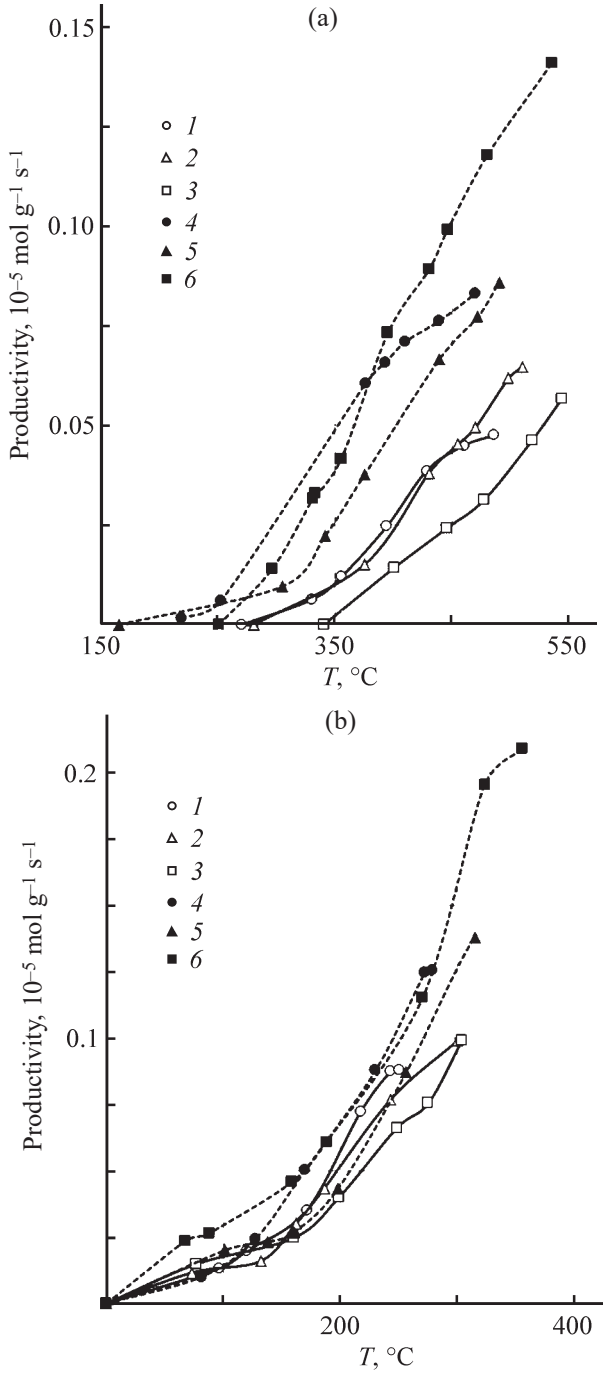

Fig. 3. Productivity of (*1*, *4*) $K_2NiTi_7O_{16}$, (*2*, *5*) $K_2MgTi_7O_{16}$, and (*3*, *6*) $K_2Al_2Ti_6O_{16}$ samples prepared by the (solid lines) solid-phase method and (dashed lines) pyrolysis of citrate–nitrate compositions in oxidation of (a) carbon monoxide and (b) hydrogen.

citrate–nitrate compositions for preparing the samples appreciably (by approximately 100°C) decreases the initial temperature of the CO oxidation (Fig. 3a), whereas in H_2 oxidation such effect is not observed

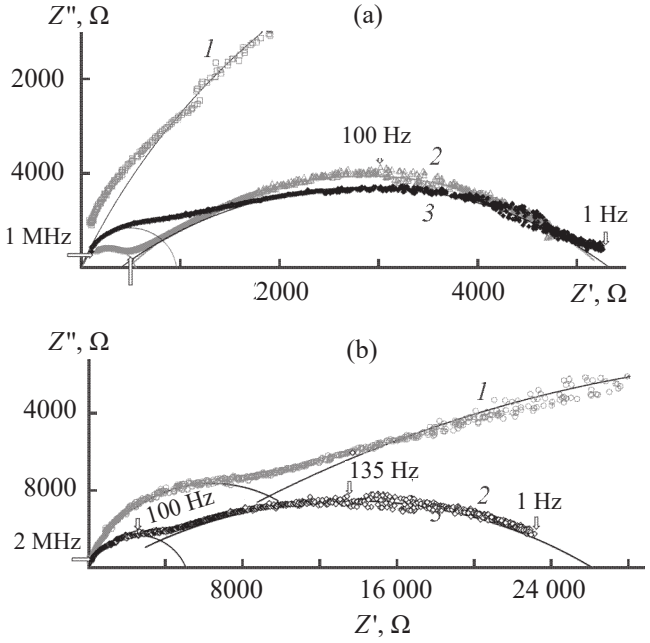

Fig. 4. (a) Impedance hodographs measured at 650°C on hollandites (*1*) $K_2MgTi_7O_{16}$, (*2*) $K_2NiTi_7O_{16}$, and (*3*) $K_2Al_2Ti_6O_{16}$; (b) Impedance hodograph measured on $K_2MgTi_7O_{16}$ at (*1*) 650 and (*2*) 700°C (presented on another scale).

(Fig. 3b). Because the oxidation of hydrogen and CO occurs by different mechanisms, it can be assumed that the pyrolysis of citrate–nitrate compositions leads to an increase in the amount of catalytically active surface sites ensuring activated adsorption of a larger amount of CO. Hence, the samples prepared by pyrolysis of citrate–nitrate compositions may be promising for use in catalytic processes, including photocatalytic wastewater treatment to remove toxic components. The aluminum-containing sample prepared by pyrolysis showed the highest catalytic activity in both model reactions (Fig. 3, curves *6*). In particular, 95% oxidation of hydrogen on this catalyst occurred at 355°C and corresponded to the performance of ~0.21×10^{-5} mol g^{-1} s^{-1}, which is 2 times higher than with the catalyst of the same composition prepared by the solid-phase method (Fig. 3b, curve *3*).

The electrotransport properties of ceramic samples prepared by the solid-phase synthesis were studied by impedance spectroscopy. Typical impedance hodographs of the compounds under consideration are shown in Fig. 4. They can be approximated by two partially overlapping hemi circles with the center lying below the abscissa. This distortion is particularly noticeable in the low-frequency part of the impedance, which is probably associated with the presence of a limited diffusion layer. In the equivalent circuit, it is described most frequently by a constant-phase element, CPE.[1] Magnesium hollandite has the lowest electrical conductivity at 650°C, $\sigma \approx 1.29 \times 10^{-5}$ S cm^{-1}; for the nickel and aluminum compounds, the corresponding values are 1.91×10^{-4} and 1.92×10^{-4} S cm^{-1}. The activation energy of the charge

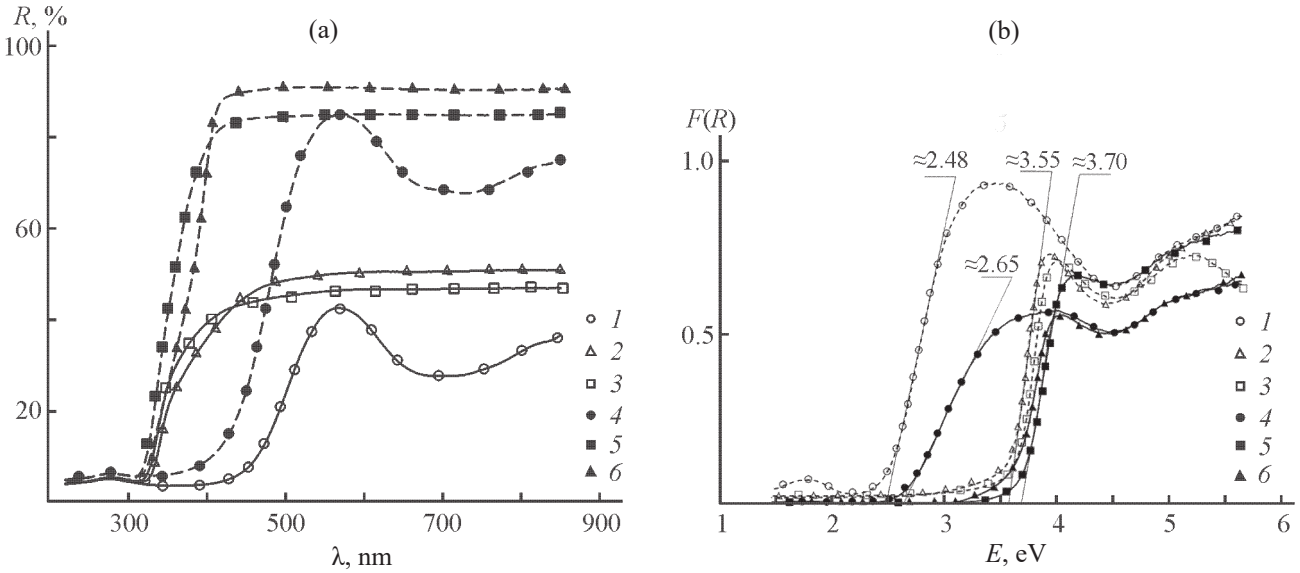

Fig. 5. (a) Diffuse reflection spectra and (b) plots of the Kubelka–Munk functions for (*1*, *4*) $K_2NiTi_7O_{16}$, (*2*, *5*) $K_2MgTi_7O_{16}$, and (*3*, *6*) $K_2Al_2Ti_6O_{16}$ samples prepared by the (solid lines) solid-phase method and (dashed lines) pyrolysis of citrate–nitrate compositions.

[1] Impedance Spectroscopy. Theory, Experiment, and Applications, Barsoukov, E. and Ross Macdonald, J., Eds., Hoboken, New Jersey: Wiley, 2005, 2nd ed., pp. 14–128.

transfer, calculated from the dependences obtained at different temperatures, is as follows: $K_2NiTi_7O_{16}$ 1.12, $K_2MgTi_7O_{16}$ 1.65, and $K_2Al_2Ti_6O_{16}$ 0.82 eV; it reasonably agrees with the published data [14].

Spectroscopic measurements (Fig. 5a) have shown that the reflection intensity of the hollandites $K_2MgTi_7O_{16}$ and $K_2Al_2Ti_6O_{16}$ in the visible and near-IR range (>400 nm) is 84 and 91%, respectively. The hollandite $K_2NiTi_7O_{16}$ exhibits two diffuse reflection peaks irrespective of the synthesis method. The dependence of the Kubelka–Munk function on the photon energy shows that the value of $F(R)$ is higher for the magnesium- and nickel-containing samples prepared by the citrate–nitrate method (Fig. 5b). This may be due to smaller particle size and, as a consequence, to stronger scattering of the incident radiation. The absorption band edges were determined for all the hollandites by the graphical method. These values can be assumed to be close to the energy of the electron transition from the valence band to the conduction band, i.e., to the band gap width (E_g). The presented plots show that E_g for the samples containing aluminum and magnesium is in the interval 3.55–3.70 eV. Only for nickel hollandite, the absorption band edge is shifted to the visible region and corresponds to the band gap width of 2.65 eV for the sample synthesized by the solid-phase method and 2.48 eV for the sample prepared by pyrolysis of citrate–nitrate compositions. Therefore, this hollandite shows promise as a photocatalyst activated with visible light.

CONCLUSIONS

The advantage of the pyrolysis of citrate–nitrate compositions over the solid-phase procedure for preparing materials of hollandite structure with the general formula $K_2Me_xTi_{8-x}O_{16}$ (Me = Mg, Ni, Al) was demonstrated. The materials prepared by pyrolysis have more developed surface and show promise as sorbents and catalysts for gas treatment. Furthermore, the $K_2NiTi_7O_{16}$ sample, also prepared by the citrate–nitrate method, has the band gap width of 2.48 eV and is therefore promising as a photocatalyst activated with visible light.

ACKNOWLEDGMENTS

The authors are grateful to Researcher N.Yu. Ul'yanova and Junior Researcher E.Yu. Brazovskaya for the assistance in studying the textural and optical characteristics of the samples (Institute of Silicate Chemistry, Russian Academy of Sciences), and also to T.A. Vishnevskaya and G.A. Galkina, who performed trials of the samples in oxidation of CO and H_2 [engineers of the St. Petersburg State Institute of Technology (Technical University), Chair of General Chemical Technology and Catalysis].

FUNDING

The study was performed within the framework of the government assignment for the Institute of Silicate Chemistry, Russian Academy of Sciences in accordance with the Basic Research Program of State Academies of Sciences for 2019–2021 (theme no. 0097-2019-0012).

CONFLICT OF INTEREST

The authors declare that they have no conflict of interest.

REFERENCES

1. Zhang, Y., Jiang, Z., Huang, J., Lim, L.Y., Li, W., Deng, J., Gong, D., Tang, Y., Lai, Y., and Chen, Z., *RSC Adv.,* 2015, vol. 97, pp. 79479–79510. https://doi.org/10.1039/C5RA11298B
2. Chen, J., Ding, T., Cai, J., Wang, Y., Wu, M., Zhang, H., Zhao, W., Tian, Y., Wang, X., and Li, X., *Appl. Surf. Sci.,* 2018, vol. 453, pp. 101–109. https://doi.org/10.1016/j.apsusc.2018.04.189
3. Zdravkov, A.V., Gorbunova, V.A., Volkova, A.V., and Khimich, N.N., *Russ. J. Gen. Chem.,* 2018, vol. 88, no. 3, pp. 528–531. https://doi.org/10.1134/S1070363218030210
4. Wang, Q., Guo, Q., and Li, B., *RSC Adv.,* 2015, vol. 5, pp. 66086–66095. https://doi.org/10.1039/c5ra10640k
5. Garay-Rodríguez, L.F., Yoshida, H., and Torres-Martínez, L.M., *Dalton Trans.,* 2019, vol. 48, pp. 12105–12115. https://doi.org/10.1039/C9DT01452G
6. Li, Q., Kako, T., and Ye, J., *Appl. Catal. A: General,* 2010, vol. 375, pp. 85–91. https://doi.org/10.1016/j.apcata.2009.12.020
7. Phoon, B.L., Lai, C.W., Juan, J.C., Show, P.-L., and Pan, G.-T., *Int. J. Hydrogen Energy,* 2019, vol. 44, no. 28, pp. 14316–14340. https://doi.org/10.1016/j.ijhydene.2019.01.166
8. Liu, X., Xu, L., Huang, Y., Qin, C., and Seo, H.J., *J. Taiwan Inst. Chem. Eng.,* 2017, vol. 76, pp. 126–131. https://doi.org/10.1016/j.jtice.2017.03.036
9. Sanford, S., Misture, S.T., and Edwards, D.D., *J. Solid State Chem.,* 2013, vol. 200, pp. 189–196.

https://doi.org/10.1016/j.jssc.2012.12.03

10. Chen, M., Wang, Z., Liu, H., Wang, X., Ma, Y., and Liu, J., *Mater. Lett.,* 2017, vol. 202, pp. 59–61. https://doi.org/10.1016/j.matlet.2017.05.072
11. Gorshkov, N.V., Goffman, V.G., Khoryukov, A.S., Sevryugin, A.V., Burmistrov, I.N., and Gorokhovskii, A.V., *Refract. Ind. Ceram.,* 2016, vol. 57, no. 4, pp. 413–416. https://doi.org/10.1007/s11148-016-9995-5
12. Gorokhovsky, A.V., Tretyachenko, E.V., Goffman, V.G., Gorshkov, N.V., Fedorov, F.S., and Sevryugin, A.V., *Inorg. Mater.,* 2016, vol. 52, no. 6, pp. 587–592. https://doi.org/10.1134/S0020168516060042
13. Khanna, S.K., Griiner, G., Orbach, R., and Beyeler, H.U., *Phys. Rev. Lett.,* 1981, vol. 47, no. 4, pp. 255–257. https://doi.org/10.1103/PhysRevLett.47.255
14. Reau, J.-M., Moali, J., and Hagenmuller, P., *J. Phys. Chem. Solids,* 1977, vol. 38, no. 12, pp. 1395–1398. https://doi.org/10.1016/0022-3697(77)90014-2
15. Liu, T., Li, Q., Xin, Y., Zhang, Z., Tang, X., Zheng, L., and Gao, P.-X., *Appl. Catal. B: Environmental,* 2018, vol. 232, pp. 108–116. https://doi.org/10.1016/j.apcatb.2018.03.049
16. Watanabe, M., Mori, T., Yamauchi, S., and Yamamura, H., *Solid States Ionics,* 1995, vol. 79, pp. 376–381. https://doi.org/10.1016/0167-2738(95)00091-J
17. Sinelshchikova, O.Y., Kuchaeva, S.K., Drozdova, I.A., Ugolkov, V.L., Petrov, S.A., and Vlasov, E.A., *Glass Phys. Chem.,* 2011, vol. 37, no. 4, pp. 433–440. https://doi.org/10.1134/S1087659611040146
18. Sinelshchikova, O.Yu., Petrov, S.A., Besprozvannykh, N.V., Kuchaeva, S.K., and Vlasov, E.A., *J. Sol–Gel Sci. Technol.,* 2013, vol. 68, no. 3, pp. 495–499. https://doi.org/10.1007/s10971-013-2988-7